Proceedings of McMat2005:
2005 Joint ASME/ASCE/SES Conference on Mechanics and Materials
June 1-3, 2005, Baton Rouge, Louisiana, USA

501

STRESS NON-UNIFORMITY IN HOLLOW CYLINDRICAL TEST SPECIMENS

P.J. Naughton
School of Engineering
Institute of Technology, Sligo, Ireland;
Ph + 353 71 9155222, Fax + 353 71 9155390,
email: naughton.patrick@itsligo.ie

B.C. O'Kelly
Department of Civil, Structural and Environmental Engineering, University of Dublin, Trinity College, Ireland; Ph + 353 1 6082387, Fax + 353 1 6773072,
email: bokelly@tcd.ie

ABSTRACT

Different levels of stress non-uniformity usually occur in test specimens of different dimensions and aspect ratios. The effect of the choice of dimensions on the level of stress non-uniformity for hollow cylindrical specimens was studied using a linear elastic analysis during the development of a new hollow cylinder apparatus. Earlier researchers have assumed slightly different variations in the stress components that act across the thickness of the specimen wall in deriving the stress equations and these differences are discussed. The current analysis assumed a linear variation in the circumferential shear stress. Slightly different regions to those reported by the other researchers were identified in generalized stress space where unacceptable levels of stress non-uniformity could arise.

The case for maintaining the confining pressures applied to the outer cell chamber and the inner bore cavity of the specimen equal to reduce the level of stress non-uniformity was also studied. It was found that stress non-uniformity could still arise when these confining pressures were maintained equal, for example when a torque was applied across the length of the specimen, with the magnitude of stress non-uniformity related to the assumed variation of the circumferential shear stress across the specimen wall. The magnitude of the calculated stress non-uniformity was shown to be related to the stress state, the specimen dimensions and the constitutive model adopted.

INTRODUCTION

The hollow cylinder apparatus (HCA) allows independent control of the magnitudes of the three principal stresses and rotation of the major-minor principal stress axes facilitating more generalized stress path testing. However, the use of the HCA in studying the constitutive behavior has often been criticized on account of the level of stress non-uniformity that may develop across the wall thickness of the hollow cylindrical test specimen. Stress non-uniformity arises due to the curvature of the specimen wall, the frictional restraint and stiffness of the annular loading platens, and whenever a torque or different confining pressures are applied across the specimen wall.

The HCA used in the present study was developed at University College Dublin (UCD), Ireland [1,2,3]. The apparatus subjects a hollow cylindrical test specimen (35.5 mm inner radius, 50.0 mm outer radius and 200 mm high) to four surface tractions: an outer cell confining pressure (p_o), an inner bore confining pressure (p_i), an axial load (W), and a torque (T), Figure 1a. Figure 1b presents the stress components (σ_z, σ_r, σ_θ, $\tau_{z\theta}$), and Figure 1c the principal stresses (σ_1, σ_2, σ_3) induced in an element of the specimen wall. Torque application causes rotation α_σ, of the $\sigma_1 - \sigma_3$ stress axes. The relative value of the intermediate principal stress σ_2, was quantified in terms of the intermediate principal stress parameter, b. The b parameter has a range of 0 to 1, with b = 0 for $\sigma_2 = \sigma_3$, and b = 1 for $\sigma_2 = \sigma_1$. The UCD HCA was closed-loop controlled [4] allowing independent and precise regulation of the system of applied loads and confining pressures.

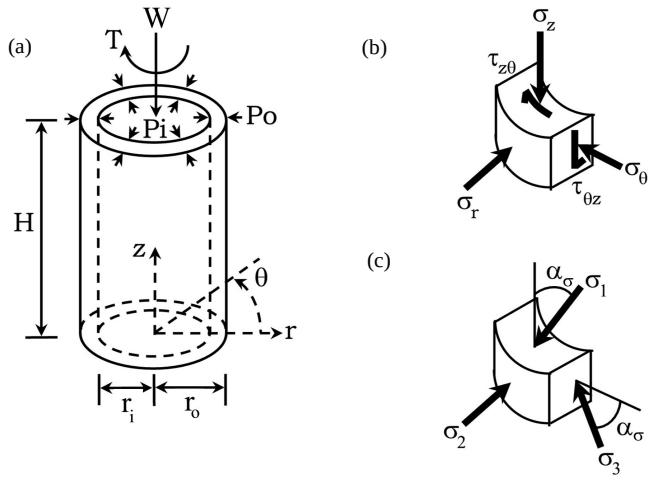

Figure 1. Stress state in hollow cylindrical specimen.

The induced stress components were computed from the applied loads and confining pressures by averaging the stresses, which were assumed to vary across the wall thickness in a particular manner, over the specimen volume. For the purposes of analysis in this study, the specimen was considered as a thick-walled hollow cylinder with an isotropic, linear elastic constitutive response. The axial, radial and circumferential normal stresses (σ_z, σ_r, σ_θ), were derived from equilibrium considerations alone, Figure 2a and 2c. The circumferential shear stress $\tau_{z\theta}$, was derived assuming a linear variation of the shear stress across the wall thickness, Figure 2b. Averaging the magnitudes of the stress components over the specimen volume resulted in the equations presented in Table 1.

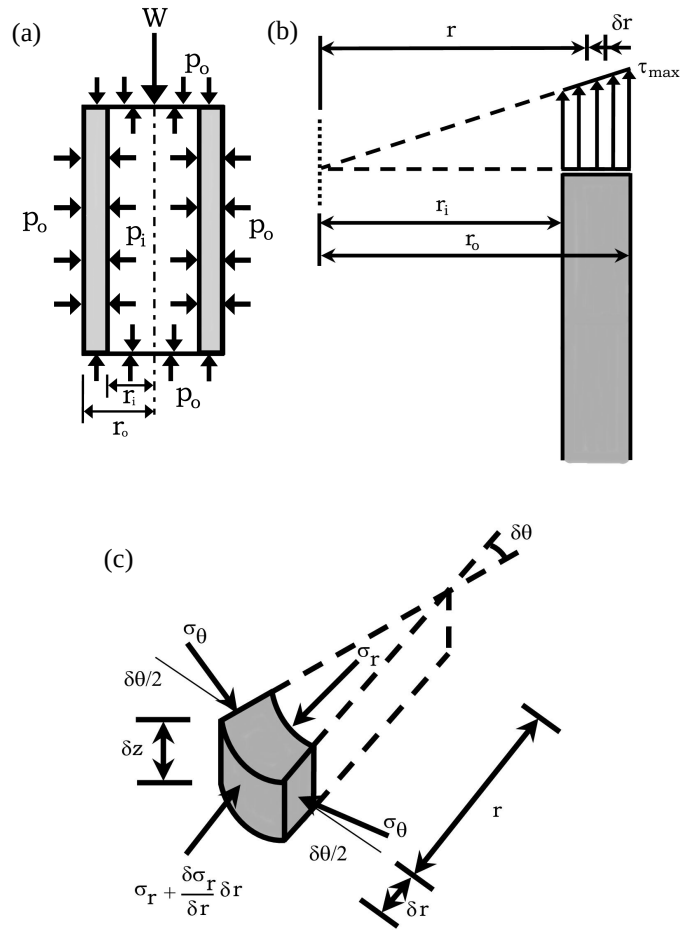

Figure 2. Assumed distribution of stresses: (a) axial, (b) circumferential shear and (c) circumferential and radial normal stresses.

QUANTIFYING STRESS NON-UNIFORMITY

The radial and circumferential normal stresses (σ_r, σ_θ), and the circumferential shear stress ($\tau_{z\theta}$) vary across the specimen wall thickness under generalized stress conditions. The axial normal stress (σ_z), may also vary depending on the assumed constitutive model, although for a linear elastic analysis the axial normal stress is uniformly distributed.

The level of stress non-uniformity was assessed using two stress non-uniformity coefficients. The β_3 stress non-uniformity coefficient [5], given by Eq 1, relates the distribution of a particular stress $\sigma(r)$, to the actual mean of that stress $\bar{s}^*$, and a measure of the stress level σ_L.

$$b_3 = \frac{\left(\int_{r_i}^{r_o} \left|s(r) - \bar{s}^*\right| \partial r\right)}{(r_o - r_i)s_L} \qquad (1)$$

The magnitude of the stress non-uniformity was considered to be unacceptable for $\beta_3 > 0.11$. In deriving the equations for the stress components [5], the circumferential shear stress was assumed to be uniformly distributed across the specimen wall thickness and resulted in $\beta_3 = 0$ for this stress component. Therefore, stress non-uniformity was only considered a function of the mean circumferential normal stress $\bar{s}_q$, and the mean radial normal stress $\bar{s}_r$, which resulted in σ_L being the mean of these two stress components.

A second stress non-uniformity coefficient β_R, has been defined in the literature [6] in terms of the major-to-minor principal stress ratio R that acts across the specimen wall thickness, Eq 2. The deformational response of granular materials including uniform sand, which was under investigation using the UCD HCA, is closely linked to R [6].

$$b_R = \frac{R_{Max} - R_{Min}}{R_{Mean}} \qquad (2)$$

where R_{Max}, R_{Min} and R_{Mean} are the maximum, minimum and mean values of the major-to-minor principal stress ratio.

A large variation in R can occur across the thickness of the specimen wall for arbitrarily chosen stress states, and assuming an elastic distribution for the different stress components. The level of stress non-uniformity was considered unacceptable for $\beta_R > 0.2$, which corresponds to a 10 % variation from the R_{Mean} value.

Table 1. Equation for mean stresses induced in the test specimen.

Axis direction	Mean stress component
Axial normal	$\bar{s}_z = \frac{W}{p(r_o^2 - r_i^2)} + \frac{p_o r_o^2 - p_i r_i^2}{r_o^2 - r_i^2}$
Radial normal	$\bar{s}_r = \frac{p_o r_o^2 - p_i r_i^2}{r_o^2 - r_i^2} - \frac{2r_i^2 r_o^2 (p_o - p_i)\ln\left(r_o/r_i\right)}{\left(r_o^2 - r_i^2\right)^2}$
Circumferen-tial normal	$\bar{s}_q = \frac{p_o r_o^2 - p_i r_i^2}{r_o^2 - r_i^2} + \frac{2r_i^2 r_o^2 (p_o - p_i)\ln\left(r_o/r_i\right)}{\left(r_o^2 - r_i^2\right)^2}$
Circumferen-tial shear	$\bar{t}_{zq} = \frac{4T(r_o^3 - r_i^3)}{3p(r_o^4 - r_i^4)(r_o^2 - r_i^2)}$

A comparison of the non-uniformity coefficients [6] indicated that for a specific specimen dimensions, the β_3 analysis would mark out a larger region in b–α_σ space where the level of stress non-uniformity was acceptable. The β_3 analysis indicated that the regions of stress space in the vicinity of (b, α_σ) = (1, 0) and (0, 90^o) would gave rise to values of β_3 > 0.11. In addition to the regions identified in the β_3 analysis, the β_R analysis also identified a region in the vicinity of $\alpha_\sigma = 45^o$ for all values of the b parameter that would result in unacceptable stress non-uniformity. This additional region was attributed to the assumptions relating to the stress distribution made in deriving the circumferential shear stress. $\tau_{z\theta}$ in the β_3 analysis was assumed to be uniformly distributed across the specimen wall thickness whereas $\tau_{z\theta}$ was assumed to increased linearly across the specimen wall in the β_R analysis.

Comparisons of the values of the stress non-uniformity coefficients determined from isotropic linear elastic analysis with those from finite element analysis using a non-linear constitutive model [7, 8], indicated that the linear elastic analysis overestimated the regions of generalized stress space where unacceptable stress non-uniformity exist. It was also concluded that β_3 = 13 % could be considered as an upper limit for defining unacceptable levels of stress non-uniformity [8].

It was not proposed to restrict the areas of generalized stress space that could be explored during the test program on uniform sand using the UCD HCA but rather to highlight test results for which unacceptable stress non-uniformity may have occurred in the specimen. An isotropic, linear elastic stress analysis was considered as a useful first stage analysis, identifying regions in generalized stress space were the levels of stress non-uniformity could be excessive. Then more detailed stress analysis would be performed to study the implications for the results of stress path tests in these regions.

STRESS NON-UNIFORMITY ACROSS SPECIMEN WALL DUE TO FRICTIONAL RESTRAINT AND STIFFNESS OF LOADING PLATENS

In the UCD HCA, the torque was applied across the length of the specimen via ribbed annular sintered bronze disks that were in contact with the specimen ends [3]. The annular discs were fitted to the top and bottom loading platens. Ideally, depending on the deformational response, slippage of the specimen ends should be able to freely occur in the radial direction. In practice, however, frictional restraint occurs at the interfaces between the annular discs and the specimen ends. Stress path tests on Toyoura sand specimens [9] indicated that the effect of frictional restraint on the deformational response was restricted to 5 mm thick zones next to the specimen ends. Hence, a non-uniform stress distribution occurred next to the specimen ends.

The rigidity of the top and bottom loading platens also induced a non-uniform distribution of the axial normal stress across the thickness of the specimen wall. This stress was concentrated near the inner and outer perimeters of the platens and reduced towards the mid-thickness of the specimen wall. Additional radial normal stress was also induced whenever the specimen had a tendency to expand or contract radially [10]. Similarly, the application of the confining pressures across the specimen wall also caused complimentary shear stresses to develop near the specimen ends. This would be particularly true for consolidated drained tests [11].

The influence of the frictional end restraint and the rigidity of the loading platens can be reduced by carefully selecting the specimen dimensions and in the design of the loading platens [12, 13]. In the UCD HCA, the specimen dimensions selected and the loading platen design minimized the potential for unacceptable stress non-uniformity [3]. Furthermore, the deformational response of the specimens were measured over its central gauge length, and these measurements were practically independent of the effects of end restrain and platen rigidity.

STRESS NON-UNIFORMITY ACROSS SPECIMEN WALL DUE TO WALL CURVATURE AND STRESS VARIATION

An analysis of the level of stress non-uniformity that acts across the wall thickness of the UCD HCA specimen was performed assuming an isotropic, linear elastic constitutive response. Regions in generalized stress space were identified where unacceptable levels of stress non-uniformity may occur.

The stress analysis was performed for a series of stress paths in R – b – α_σ space considering the UCD HCA specimen as a single element, Figure 3. The mean confining stress p, remained fixed at 500 kPa, which corresponded to the mid range for any particular test performed using the apparatus. The level of stress non-uniformity was independent of the value of p since the axial normal stress was assumed to be uniform across the specimen wall in this analysis. While this assumption was not strictly correct due to frictional end restraint effects, it was assumed that the axial normal stress would be uniform over the central gauge length of the specimen. The stress paths consisted of increasing R, while p, b and α_σ remained constant, Figure 3. The stress paths originated from the b–α_σ plane, with b increasing in steps of 0.25 from b = 0 to 1, and with α_σ increasing in steps of 22.5^o from α_σ = 0 to 90^o. These stress paths were analyzed for R = 1.5, 2.0, 2.5, 3.0 and 3.5.

The inner (r_i) and outer (r_o) radii of the specimen were assumed to remain fixed at their initial values of 35.5 and 50.0 mm, respectively, for the purposes of the stress analysis. The error introduced by this assumption was acceptable for the test program on uniform sands at small and intermediate strain levels.

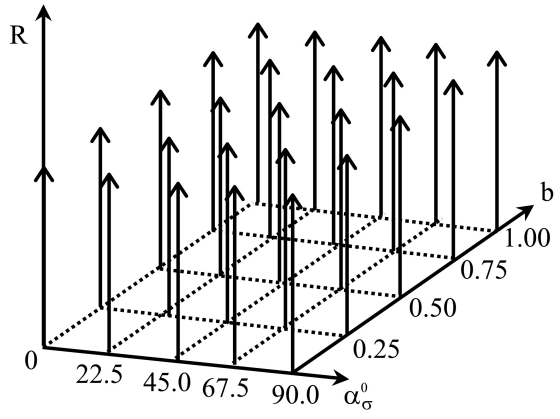

Figure 3. Stress paths studied for the UCD HCA.

The magnitudes of the applied loads and confining pressures that corresponded to different points on the stress paths were calculated using the equations presented in Table 1. These values were then used to calculate the magnitudes of the stress components and the principal stresses for different radii r, in the range $r_i \le r \le r_o$. The stress components (σ_r^r, σ_θ^r, $\tau_{\theta z}^r$, σ_z^r) corresponding to a particular radius r, were calculated using the Lamé equations, Eqs 3, 4, 5 [15], from which the three principal stresses, R and the coefficient β_R were determined.

$$\begin{matrix} s_r^r \\ s_q^r \end{matrix} = \frac{P_o r_o^{\,2} - P_i r_i^{\,2}}{r_o^{\,2} - r_i^{\,2}} \mp \frac{r_o^{\,2} r_i^{\,2}\left(P_o - P_i\right)}{\left(r_o^{\,2} - r_i^{\,2}\right) r^2} \qquad (3)$$

$$t_{qz}^r = \frac{2T}{p\left(r_o^{\,4} - r_i^{\,4}\right)} r \qquad (4)$$

$$s_z^r = s_z \qquad (5)$$

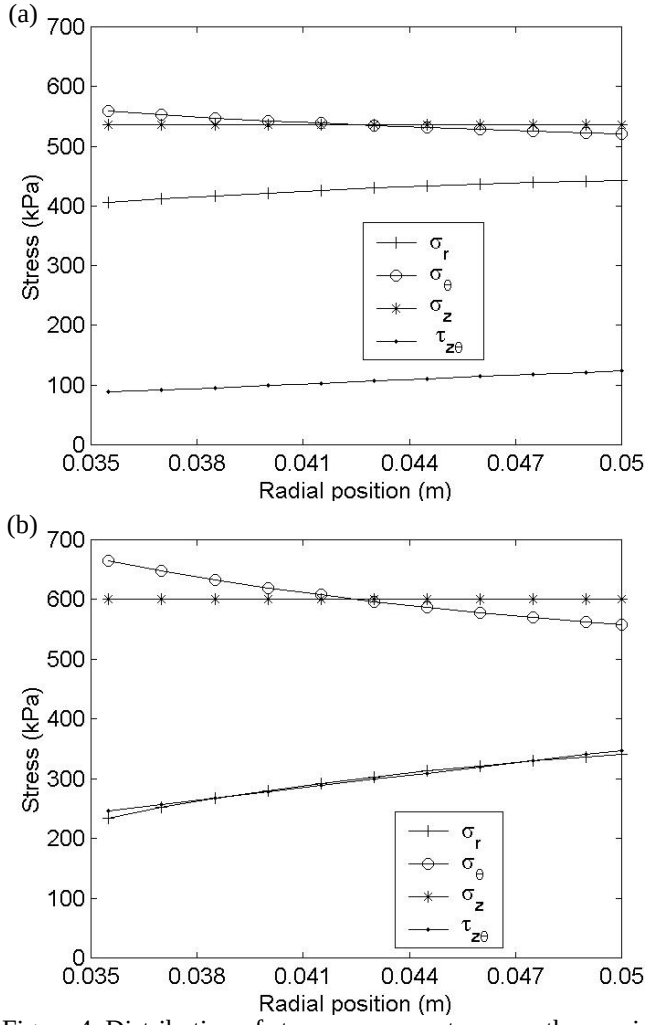

Figure 4. Distribution of stress components across the specimen wall for (R, b, α_σ) stress states of (a) 1.5, 0, 45° and (b) 3.0, 0, 45°), respectively.

Typical distributions of the stress components across the specimen wall thickness are presented in Figure 4a and b for two arbitrarily chosen stress states of (R, b, α_σ) = (1.5, 0, 45°) and (3.0, 0, 45°), respectively, with the variation in R across the specimen wall presented in Figure 5.

DISCUSSION OF RESULTS

The magnitude of the β_R coefficient was found to be greatly affected by that of the major-to-minor principal stress ratio R with acceptable levels of stress non-uniformity throughout b–α_σ stress space for R < 1.5, Figure 6a. However, unacceptable levels of stress non-uniformity occurred in certain regions of b–α_σ space for R > 1.5, Figure 6b, and the size of these regions was found to increase with increasing R values. These regions, shown schematically in Figure 7, were generally located in the vicinity of b = 1, α_σ = 0°, R > 1.5 and b = 0, α_σ = 90°, R > 3.0 in generalized stress space. A third region was also identified in the vicinity of α_σ = 45° for all values of the b parameter where unacceptable levels of stress non-uniformity could potentially occur for R > 1.5.

The regions identified in Figure 7 were similar to those reported by [6] apart from the following exceptions: the magnitude of β_R was considerably smaller in the vicinity of b = 0, α_σ = 90°, and larger in the vicinity of b = 1.0, α_σ = 0° for all of the R values studied. The highest level of stress non-uniformity identified in the current analysis occurred in the vicinity of b = 1.0, α_σ = 0°. The discrepancy between the results of this stress analysis and that reported by [6] may be explained by the different specimen dimensions used in the two studies. The specimen analyzed in [6] had larger inner and outer radii of 51.0 and 76.0 mm, which resulted in a thicker specimen wall of 25 mm compared to that of 14.5 mm for the UCD HCA specimen. The magnitude of the β_R coefficient was found to be influenced by both the wall thickness, reducing as the wall thickness reduced, and by the difference in the confining pressures applied to the outer cell chamber and the inner bore cavity of the specimen [6]. The difference in the confining pressures that acted across the specimen wall was a function of the inner specimen radius, and reduced as the inner radius increased when p, b and α_σ remained constant.

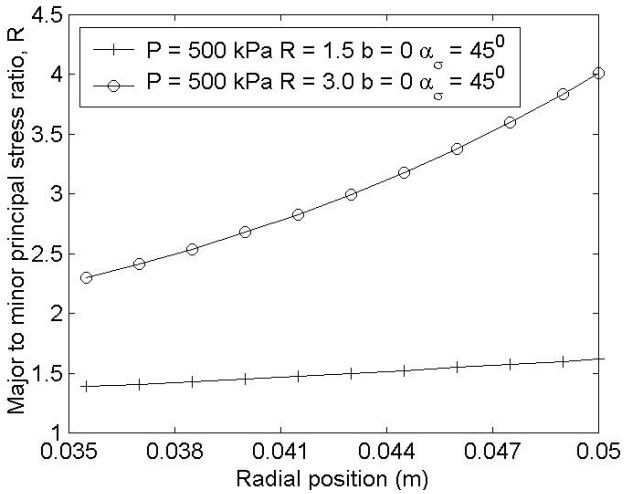

Figure 5. Variation of the major-to-minor principal stress ratio for (R, b, α_σ) equal to (a) 1.5, 0, 45°, and (b) 3.0, 0, 45°.

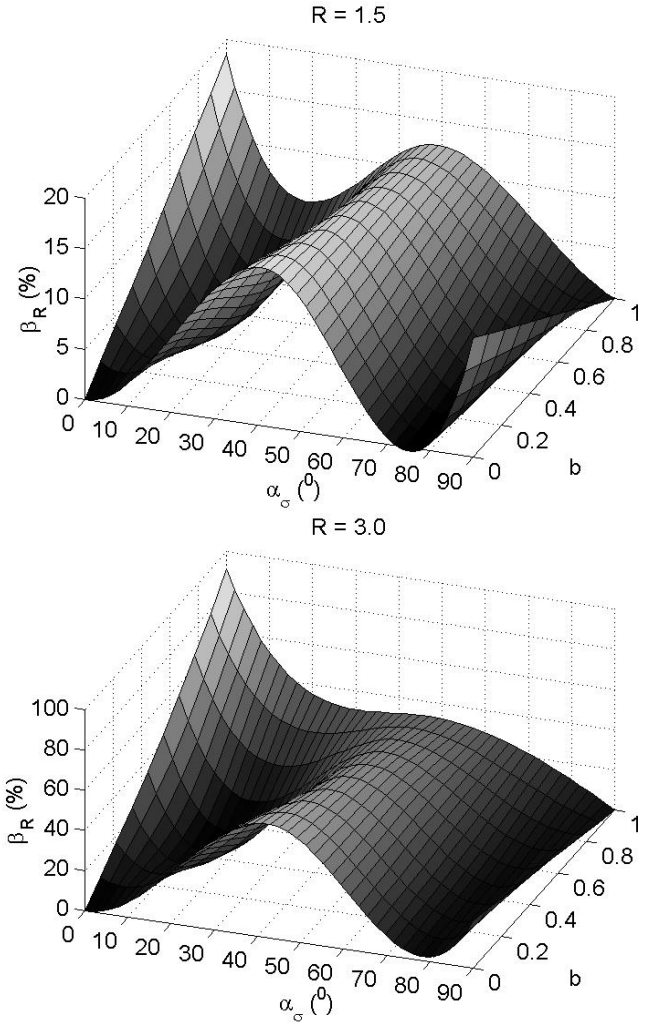

Figure 6. Variation of β_R in b–α_σ stress space for (a) R = 1.5 and (b) R = 3.0.

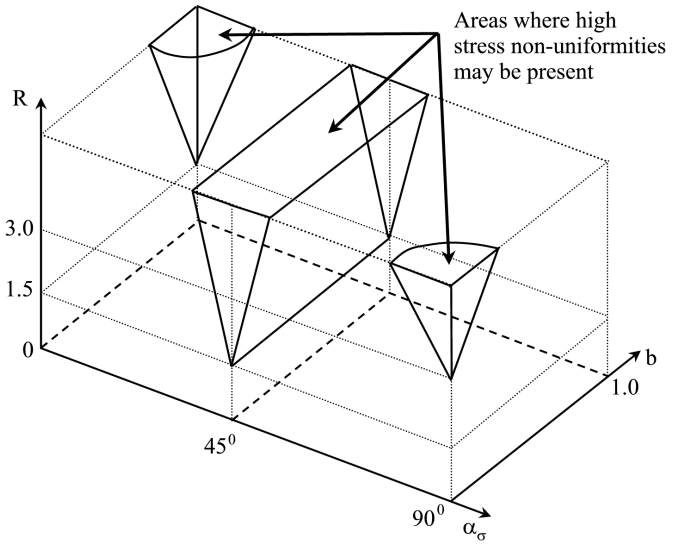

Figure 7. Regions in generalized stress space where unacceptable levels of stress non-uniformity could occur.

INFLUENCE OF CELL AND BORE CONFINING PRESSURES ON STRESS NON-UNIFORMITY

The level of stress non-uniformity was influenced by the difference in the confining pressures applied to the outer cell chamber and the inner bore cavity of the specimen [5, 10, 14]. In an attempt to control the level of stress non-uniformity, several researchers including [10, 14] have recommended maintaining $p_o = p_i$, thereby ensuring that σ_r or σ_θ could not vary across the specimen wall thickness. Other researchers including [5] recommended that the ratio of the confining pressures should be restricted within the range $0.9 \le p_o/p_i \le 1.2$.

A scatter plot of β_R versus p_o/p_i for the stress paths analyzed in this study indicated that a significant number the stress states located outside the limits of $0.9 \le p_o/p_i \le 1.2$ and $\beta_R < 20$ %, Figure 8. These stress states are located in the vicinity of (b, α_σ) = (1, 0^o) and (0, 90^o), and $\alpha_\sigma = 45^o$ for $0 \le b \le 1$, and these regions have been identified earlier as areas of unacceptable stress non-uniformity. Unacceptable levels of stress non-uniformity only developed for $R > 2.0$ with $p_o = p_i$. However, the regions of generalized stress paths that can be probed using the HCA are also restricted to $b = \mathrm{Sin}^2\alpha_\sigma$ [6] by enforcing the condition of $p_o = p_i$.

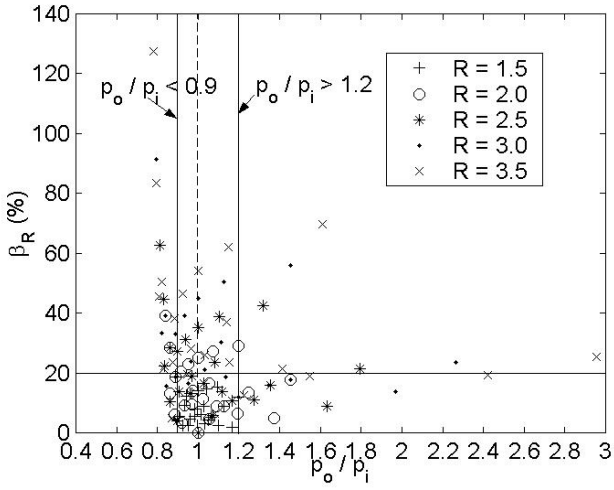

Figure 8. Variation of β_R with confining pressure ratio p_o/p_i.

CONCLUSIONS

Stress non-uniformity generally developed across the wall thickness of hollow cylindrical test specimens. Finite element analysis assuming an isotropic, linear elastic response was found to overestimate the actual level of stress non-uniformity present in the specimen but was still considered as a useful first stage analysis. The magnitude of the calculated level of stress non-uniformity acting across the thickness of the specimen wall depended on the stress state, the specimen dimensions and the constitutive model adopted.

The level of stress non-uniformity produced by frictional restraint that occurred at the specimen ends could be reduced considerably by careful design of the annular loading platens and by measuring the deformational response of the specimen over its central gauge length.

An isotropic, linear elastic stress analysis identified three different regions in generalized stress space where unacceptable levels of stress non-uniformity could develop. These regions were located in the vicinity of:

- $(b, \alpha_\sigma) = (0, 90^o)$ for $R > 3.0$,
- $(b, \alpha_\sigma) = (1, 0^o)$ for $R > 1.5$,
- $b = 0$ to 1, $\alpha_\sigma = 45^o$ for $R > 1.5$.

The size of these regions was a function of the major-to-minor principal stress ratio R, and increased with increasing R values.

When the circumferential shear stress was assumed to vary linearly across the thickness of the specimen wall, the analysis indicated that the level of stress non-uniformity was not significantly reduced by placing restrictions on the ratio of the confining pressures applied to the outer cell chamber and the inner bore cavity of the specimen. The regions of generalized stress space that can be probed using the HCA were further restricted to $b = Sin^2\alpha_\sigma$ when the confining pressures applied to the outer cell chamber and the inner bore cavity were maintained equal.

The philosophy adopted in the use of the UCD HCA was not to place restrictions on the regions of generalized stress space that could be probed but rather to mark stress paths that may have been affected by unacceptable levels of stress non-uniformity for further analysis.

ACKNOWLEDGMENTS

The research was carried out by the authors towards PhD degrees at University College Dublin, Ireland. The support of Tom Widdis and Eugene O'Brien is gratefully acknowledged. The second author would also like to acknowledge funding through the Pierse Newman Scholarship in Civil Engineering from University College Dublin.

REFERENCES

[1] O'Kelly, B.C. & Naughton, P.J., 2003, "Development of the University College Dublin hollow cylinder apparatus", *Proceedings of the 56th Canadian Geotechnical Conference*, Winnipeg, 29 September–01 October, CD Rom.

[2] O'Kelly, B.C. & Naughton, P.J., 2003, "Development of a new hollow cylinder apparatus for generalised stress path testing", *Ground Engineering*, **36, 7**, pp. 26–28.

[3] O'Kelly, B.C. & Naughton, P.J., 2005, "Development of a new hollow cylinder apparatus for stress path measurements over a wide strain range", *Geotechnical Testing Journal*, **28**, 4.

[4] O'Kelly, B.C. & Naughton, P.J., 2005, "Closed loop control of a hollow cylinder apparatus", *Proceeding of the Joint ASME/ASCE/SES Conference on Mechanics and Materials*, June 1-3, 2005, Baton Rouge, Louisiana, USA.

[5] Hight, D.W., Gens, A. & Symes, M.J., 1983, "The development of a new hollow cylinder apparatus for investigating the effects of principal stress rotation in soils", *Geotechnique*, **33**, pp. 355–383.

[6] Sayao, A. & Vaid, Y.P., 1989, "A critical assessment of stress nonuniformities in hollow cylinder test specimens", *Soils and Foundations*, **31**, pp. 60–72.

[7] Wijewickreme, D. & Vaid, Y.P., 1991, "Stress nonuniformities in hollow cylinder torsional specimens", *Geotechnical Testing Journal*, **14**, pp. 349–362.

[8] Menkiti, O.C., 1995, "Behaviour of clay and clayey sand, with particular reference to principal stress rotation", Ph.D. thesis, University of London (Imperial College).

[9] Tatsuoka, F., Ochi, K., Fujii, S. and Okamoto, M., 1986, "Cyclic undrained triaxial and torsional shear strength of sands for different sample preparation methods", *Soils and Foundations*, **26**, pp. 23–41.

[10] Saada, A.S., Fries, G. & Ker, C-C., 1983, "An evaluation of laboratory testing techniques in soil mechanics", *Soils and Foundations*, **23**, pp. 98–112.

[11] Talesnick, M. and Frydman, S., 1991, "Simple shear of an undisturbed soft marine clay in NGI and torsional shear equipment", *Geotechnical Testing Journal*, **14**, pp. 180–194.

[12] Saada, A.S. & Townsend, F.C., 1981, "State of the art: Laboratory strength testing of soils, "*Laboratory shear strength of soil*, ASTM STP740, pp. 7–77.

[13] Vaid, Y.P., Sayao, A., Hou, E. & Negussey, D., 1990, "Generalized stress path dependent behaviour with a new hallow cylinder torsional apparatus", *Canadian Geotechnical Journal*, **27**, pp. 601–616.

[14] Saada, A.S., 1988, "Hollow cylinder torsional devices: Their advantages and limitations", *Advanced Triaxial testing of Soils and Rocks, ASTM STP 977*, pp. 766–795.

[15] Boresi, A.P., Schmidt, R.J. & Sidebottom, O.M., 1993, "Advanced mechanics of materials", John Wiley & Sons, New York, pp. 444–447.